Supplement of Atmos. Chem. Phys., 19, 6843–6859, 2019
https://doi.org/10.5194/acp-19-6843-2019-supplement

Atmospheric Chemistry and Physics
Open Access
EGU

Supplement of

Submicron aerosol composition in the world's most polluted megacity: the Delhi Aerosol Supersite study

Shahzad Gani et al.

Correspondence to: Joshua S. Apte (jsapte@utexas.edu) and Lea Hildebrandt Ruiz (lhr@che.utexas.edu)

Table S1. Summary annual (2017) and campaign (January 2017 to April 2018) statistics including arithmetic mean (AM), geometric mean (GM), geometric standard deviation (GSD) and synthetic AM for hourly data of various species. Synthetic AM was calculated using the averages of the six 2-month periods (January-February through November-December). $PM_{2.5}$ data from R.K. Puram (DPCC) with only partial data for April-2017. Composition-based estimate of PM_1 (C-PM_1) = BC + NR-PM_1.

	Annual (2017)				Campaign (Jan-2017 to Apr-2017)			
	AM	GM	GSD	Synthetic AM	AM	GM	GSD	Synthetic AM
$PM_{2.5}$	140	104	2.2	139	147	113	2.2	145
C-PM_1	108	80	2.2	115	125	93	2.3	117
NR-PM_1	84	59	2.3	101	101	70	2.4	103
Org	49	33	2.5	60	60	41	2.5	62
Chl	5.8	1.0	6.5	7.9	9.0	1.6	7.3	8.5
NH_4	8.8	6.0	2.4	10	10	6.6	2.6	10
NO_3	8.5	4.4	3.3	11	11	5.6	3.4	11
SO_4	12	9.6	1.9	12	12	9.5	1.9	11
BC	12	8.9	2.3	12	12	8.5	2.3	11

Table S2. Relative ionization efficiency (RIE) for ammonium and sulfate and response factor for nitrate for the two periods of this study.

	NH_4 RIE	SO_4 RIE	NO_3 RF
Jan-Sep 2017 (average)	7.07	1.04	5.09×10^{-11}
Dec-Apr 2018 (based on calibration in Jan 2018)	9.44	1.37	5.27×10^{-11}

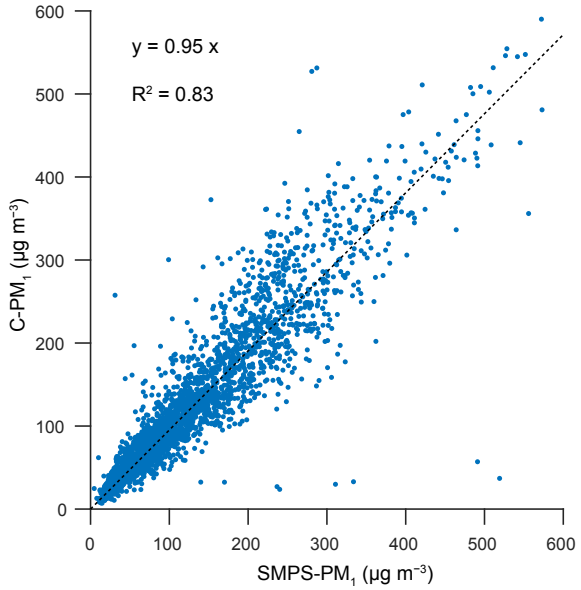

Figure S1. Scatter plot between C-PM_1 (Composition-PM_1 = NR-PM_1 + BC) and SMPS-PM_1 (PM_1 mass concentration estimated using PSD and assuming a density of 1.6 g cm^{-3}).

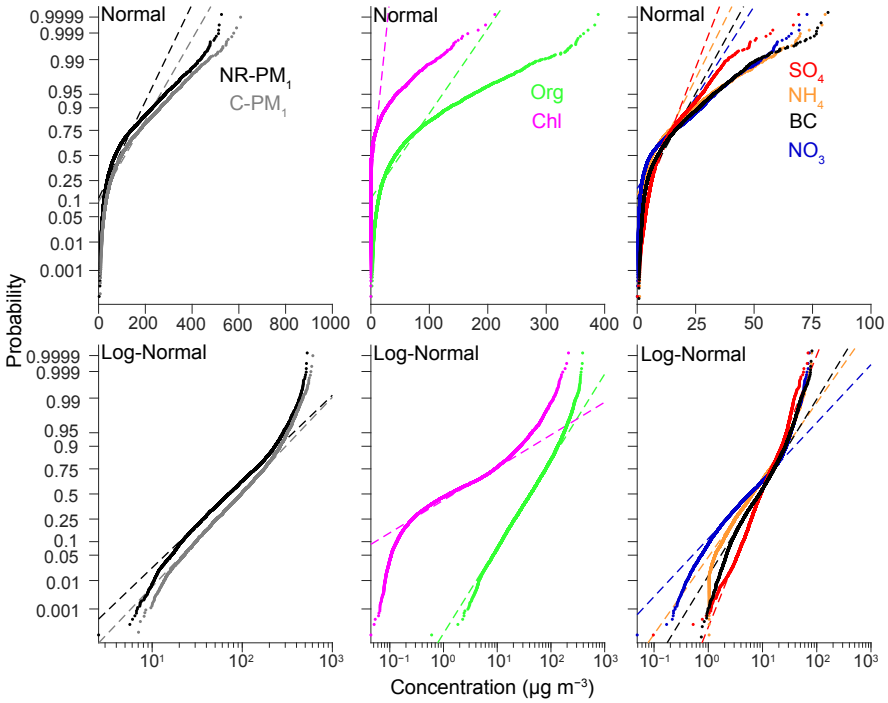

Figure S2. Probability plots for NR-PM_1, C-PM_1, Org, Chl, SO_4, NH_4, BC and NO_3 assuming normal and log-normal distributions. The dashed line represents what a normally (1st row panels) or log-normally (2nd row panels) distributed data would look like. Composition-based estimate of PM_1 (C-PM_1) = BC + NR-PM_1.

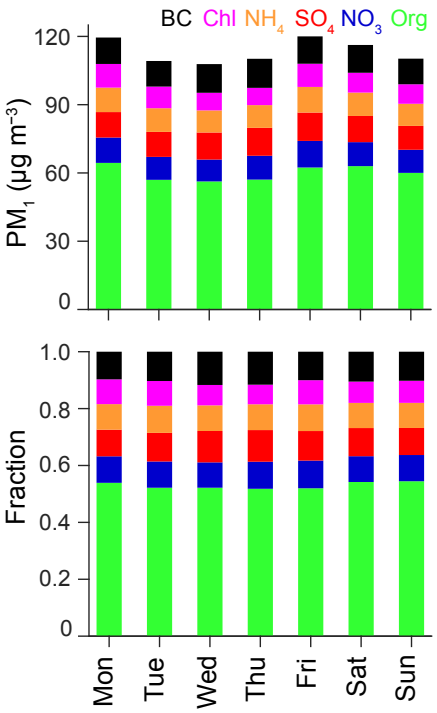

Figure S3. Average absolute and fractional composition of C-PM_1 (NR-PM_1 + BC) by day of week.

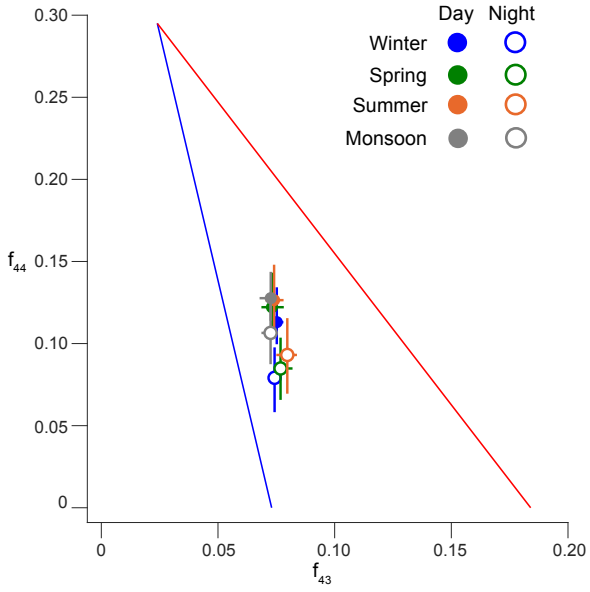

Figure S4. Average values for f_{43} and f_{44} included in the Ng et al. (2011) triangle plot. The horizontal and vertical lines are the 25th (left and bottom) and 75th percentiles (right and top).

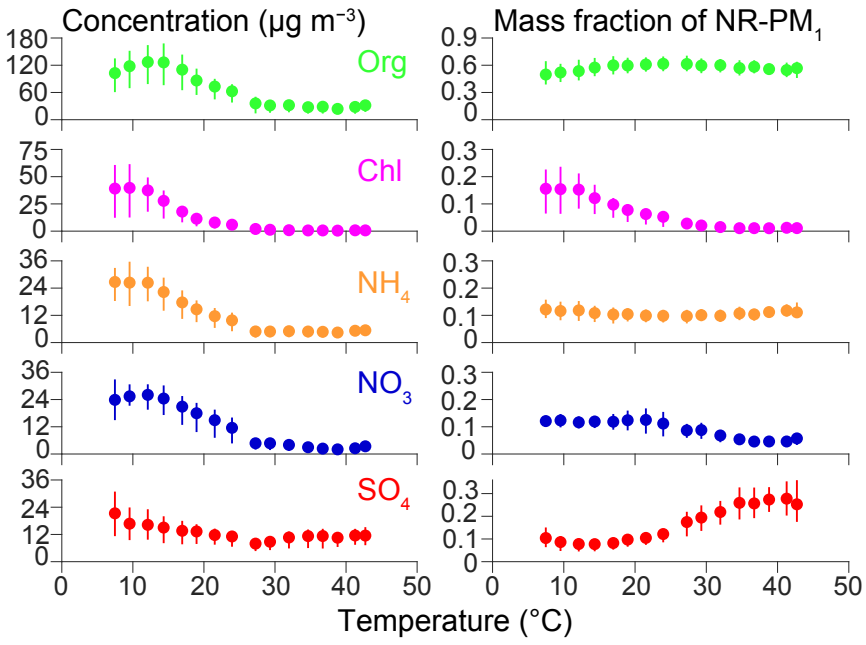

Figure S5. Variations of mass fractions of NR-PM1 species as a function of temperature. The data were binned according to the temperature, and the vertical lines are the 25th (bottom) and 75th (top) percentiles.

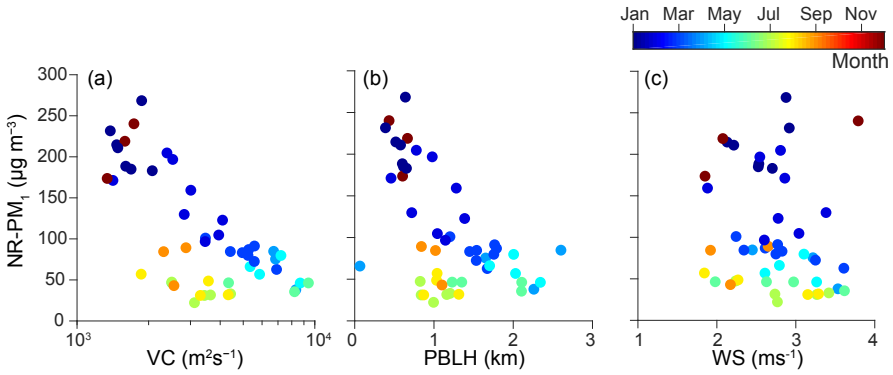

Figure S6. Variations of NR-PM_1 mass concentrations as a function of (a) ventilation coefficient, (b) planetary boundary layer height and (c) wind speed. Each scatter point is a weekly average and is color-coded with the month. Note that July to mid-September is the monsoon season.

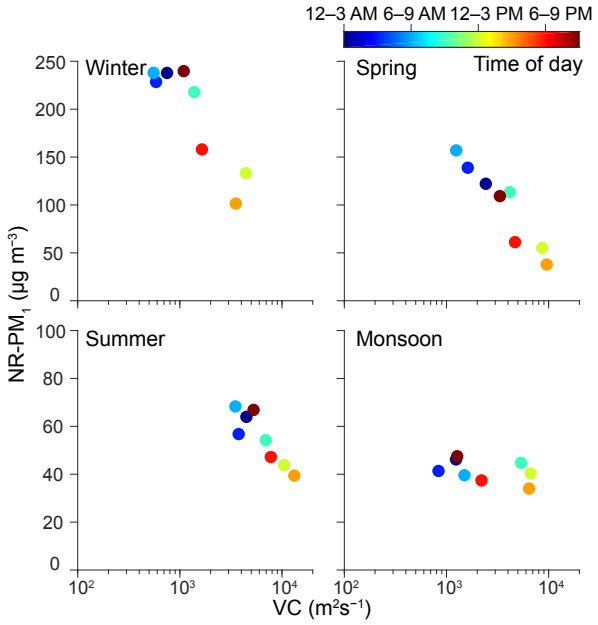

Figure S7. Variations of NR-PM_1 mass concentrations as a function of ventilation coefficient by season. Each scatter point is the average value for a day segment (color-coded).

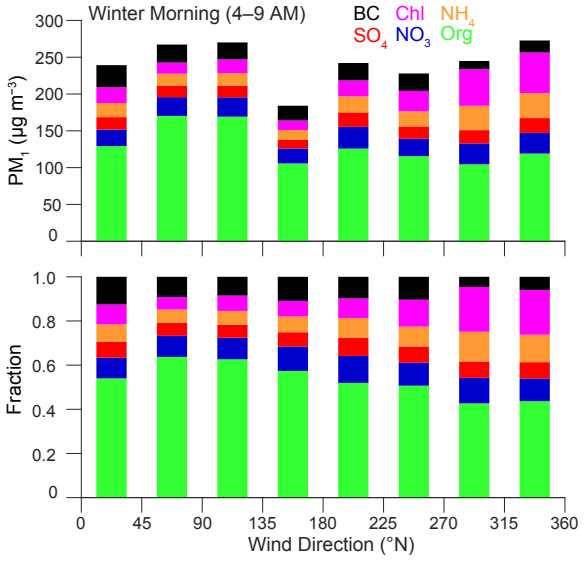

Figure S8. Average absolute and fractional composition of C-PM_1 (NR-PM_1 + BC) by wind direction for winter morning (4–9 AM)—when chloride concentrations were generally high. Chloride mass and fractional concentrations were higher when winds were from the northwest.

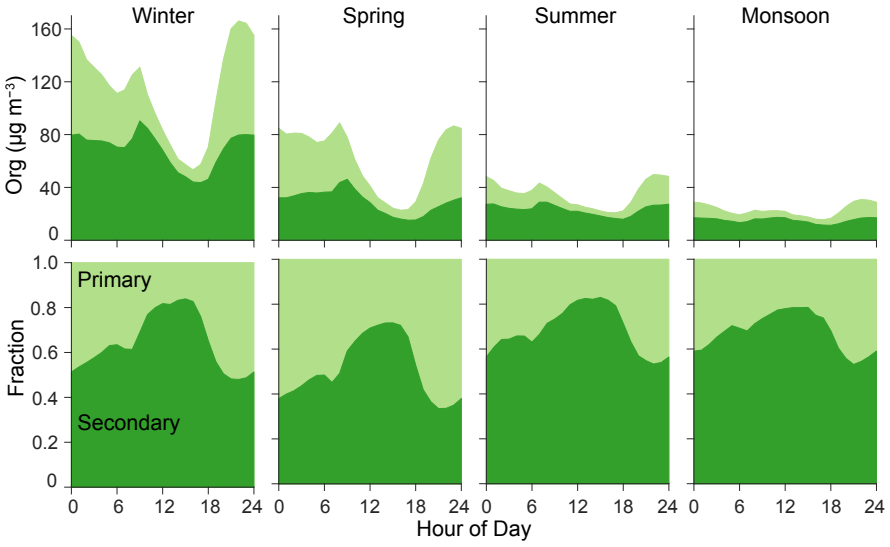

Figure S9. Average diurnal variation of mass concentrations and mass fractions of primary organic aerosol and secondary organic aerosol by season.

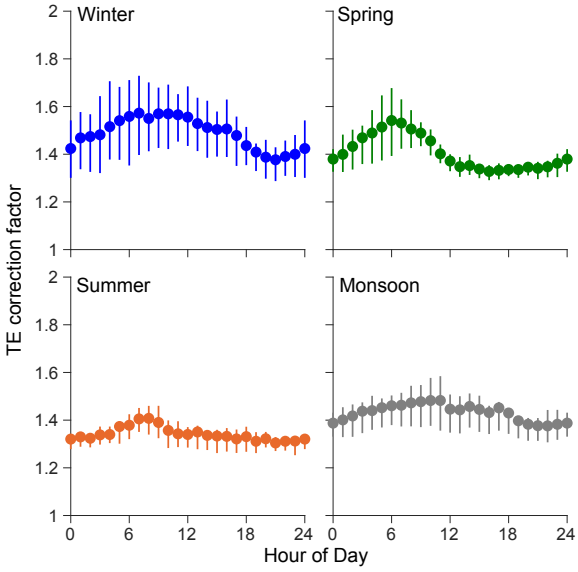

Figure S10. Diurnal variation in average transmission efficiency by season and time of day. The vertical lines are the 25th (bottom) and 75th (top) percentiles.

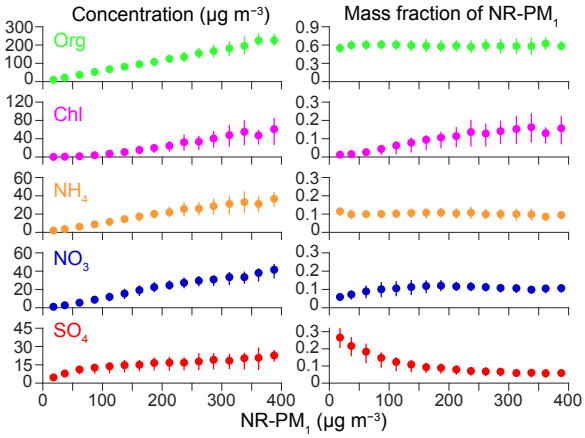

Figure S11. Variations of mass concentrations and mass fractions of NR-PM1 species as a function of NR-PM_1 mass loadings. The data were binned according to the total NR-PM1 mass, and the vertical lines are the 25th (bottom) and 75th (top) percentiles.

References

Ng, N. L., Canagaratna, M. R., Jimenez, J. L., Chhabra, P. S., Seinfeld, J. H., and Worsnop, D. R.: Changes in organic aerosol composition with aging inferred from aerosol mass spectra, Atmospheric Chemistry and Physics, 11, 6465–6474, https://doi.org/10.5194/acp-11-6465-2011, 2011.